Model. Earth Syst. Environ. (2016) 2:207
DOI 10.1007/s40808-016-0261-0

ORIGINAL ARTICLE

A mathematical method and artificial neural network modeling to simulate osmosis membrane's performance

E. S. Salami[1] · M. Ehetshami[2] · A. Karimi-Jashni[1] · M. Salari[1] · S. Nikbakht Sheibani[3] · A. Ehteshami[4]

Received: 9 November 2016 / Accepted: 23 November 2016 / Published online: 30 November 2016

Abstract Lack of fresh water has been a major obstacle to development and flourishing in human history. Desalination provides a new vision toward fresh water production in the upcoming future. The study has proposed a simple mathematical equation and ANN models to simulate eight types of sea water RO membranes. The Artificial Neural Network (ANN) models have been developed to simulate TDS corresponding to the temperature (T, °C), flow rate (gpm) and recovery percentage. The feed data was generated by ROSA software. The model developed using a simple rational mathematical method. ANN models were trained using feed-forward back propagation algorithm with two hidden layers and various numbers of neurons in each layer. The model verification analysis proved both mathematical and ANN models to be highly accurate, reliable and practical for analyzing, designing, operating and optimizing of RO systems. The correlation coefficients (R) of 0.96 and 0.97, respectively, confirmed that the equation and ANN models resulted in this study are in good agreement with the measured data.

Keywords Artificial neural network · Desalination · Modeling · Osmosis membranes · ROSA

✉ M. Ehetshami
Maehtesh@gmail.com

E. S. Salami
Esisalami@yahoo.com

A. Karimi-Jashni
Ajashni@yahoo.ca

M. Salari
Salari.marjan@gmail.com

S. Nikbakht Sheibani
Solmaznikbakht87@yahoo.com

A. Ehteshami
Ehteshami@ce.sharif.edu

[1] Environmental Engineering Department, Shiraz University, Shiraz, Iran

[2] Environmental Engineering Department, KN Toosi University of Technology, P. O. Box 1587-544-16, Tehran, Iran

[3] CE, Apadana University, Shiraz, Iran

[4] CE Department, Sharif University of Technology, Tehran, Iran

Introduction

Fresh water is one of the most essential and vital necessities of human and other living creatures. However, less than one percent of available water is fresh, while 97% is in the oceans and 2% is in ice form (Clayton 2011). Models can act as a considerable amount of illustration for simplifying the complicated hydrogeological occurrences in water resources assessment strategy (Ehteshami et al. 1991; Salami Shahid and Ehteshami 2015, 2016; Ebrahimi et al. 2015; Ehteshami and Biglarijoo 2014). A possible solution to the shortage of fresh water is desalination of seawater or brackish water which is freely available nearby coastal lands (Zirakrad et al. 2013). Desalination processes produce a stream of freshwater, and a separate, saltier stream of water that requires disposal (Carter 2015; Crittenden et al. 2005; Zirakrad et al. 2013). Greenlee et al. (2009) studied system performance variation and impacts of using brackish or sea water for desalination by RO systems.

There are several different methods for desalination such as thermal and membrane methods. Thermal methods separate water by evaporation and condensation whereas membrane processes use semi-permeable membranes for

the separation (Venkatesan 2014). Application of reverse osmosis membranes is the most viable method for desalination today. Furthermore, using RO membrane for wastewater treatment is swiftly expanding (Garud et al. 2011). Low cost, energy efficiency and versatility of the process, in comparison with other technologies are some of its advantages (Abraham 2005; Nakayama and Sano 2013; Stover 2013). RO systems also provide an adequate capability of strong separation (Pangarkar et al. 2011). Its concept is known and studied from 1748 by many scientists, however, as a feasible separation process, it is a relatively young technology (Williams 2003). In addition to desalination of sea and brackish water, RO systems also remove dissolved solids, organic, pyrogens, submicron colloidal matter, color, nitrate and bacteria from water/wastewater (Garud et al. 2011). System structure details of RO are briefly explained by many researchers such as (Crittenden et al. 2005; Hiroki 2010; Williams 2003). The RO systems efficiency, described as E in Eq. 1, depends on three main types of factors such as: design details of the plant and operation conditions, quantity and quality characteristics of influent S_o and outflow S_e, and type of the membranes used in the RO system (Crittenden et al. 2005; Hiroki 2010; Williams 2003).

$$E(\%) = 1 - \frac{S_e}{S_0} \quad (1)$$

This study focuses on the performance of eight different types of SWRO membranes with one pass and one stage in each pass. As it is shown in Fig. 1, no feed/back pressure is applied added before and after SWRO element.

Reverse Osmosis System Analysis (ROSA) software was used to produce data required for the study. ROSA software has been developed by Dow Chemical Company (ROSA 2010). Many researchers have used the software for modeling or comparing their models predictions with ROSA's simulation results (Afrasiabi et al. 2009; Chen and Li 2005; Gedam et al. 2012). A correlation of 85% was obtained, comparing the developed model and ROSA software results (Jafar and Zilouchian 2002). Jiang et al. (2014) used several mathematical methods to find the relations between temperature and feed pressure and performance of a SWRO plant. They focused on and paid special attention to details of working parameters and differential changes in operational variables. Patroklou (2013) tried to model the effect of pH, temperature and pressure on boron concentrations at the end of RO processes, using RE4040-SR membrane, through a mathematical relation based on a solution of a diffusion model. Arulchinnappan, presented a multivariate fuzzy regression model to simulate RO process conditions (Arulchinnappan and Rajendran 2011). Artificial neural network (ANN) presented by (Libotean et al. 2009; Abbasi Maedeh et al. 2013) used numerous daily performance data as inputs to simulate permeate flux and salt passage. A two-dimensional (2-d) mathematical model (computational fluid dynamics and biofilm models) was used by Radu et al. (2010) to describe the negative effects of biofilm growth on the performance of a spiral-wound reverse osmosis which indicates the importance of RO system performance monitoring.

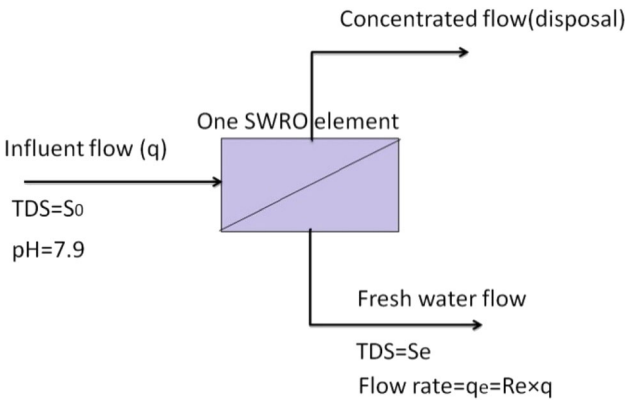

Fig. 1 Design of one stage one pass desalination system used in the study

Almost all researchers in this field have faced the performance analyses such as the study done by Harrak et al. (2013). They suggested removing chlorination and sodium bisulfite addition steps from the pretreatment to reach an acceptable performance. Kumar and Saravanan (2011) and Gedam et al. (2012) compared the recovery rate, TDS reduction, energy consumption and investment cost of a ROSA type membrane, with a KOCH type membrane for treatment of effluent from knitted fabric dyeing and showed that the KOCH membranes work better. Stover, (2013) tried to show how better performances are accessible in a closed circuit or semi-batch RO techniques. Al-Mutaz (2003) and Abraham (2005) showed that coupled systems consist of RO and multi-stage flash (MSF) have the best wastewater desalination performance.

The main goal of this study is to represent mathematical equations and also artificial neural network (ANN) models for estimating effluent total suspended solids (TDS), fresh flow concentration, (Se), of a treated saline water with influent concentration of (S0), temperature (T), recovery percentage (Re) and influent flow (q). The developed models and equations are calibrated for 8 different types of sea water RO membranes (SWRO). Both methods of modeling (ANN and mathematical equation) have accurate and reliable results, while each method has its advantage that can be very useful for the application of SWRO systems.

Strategy and procedure

RO desalination procedure, SWRO membranes

Table 1 shows eight types of SWRO membranes that are used in this study and also the boundary conditions for each RO element. Maximum recovery percentage (Re) is limited to 15% and temperature is up to 46 °C for each element.

Other researchers have tried to model the RO performance systems, like Altaee (2012) who presented a mathematical model for two types of SW30HRLE-440i and SW30HR-380 in TDS ranges of 32,000, 35,000, 38,000, and 43,000 mgL^{-1}.

Efficiency (E) is the best parameter to indicate the system performance. The main goal of present study is to find a simple mathematical model/equation and ANN models for predicting Se by knowledge of S0, T, Re, and q. The highlight of this study is to present an equation and/or model(s) for 8 types of SWRO membranes, while the most of preceding research works include only one or two RO membrane types. The main parameters that affect the efficiency of RO systems are the properties of influent water, including: T, q, TDS and operational conditions such as the pressure, which has a major impact on RO performance (Gedam et al. 2012; Harrak et al. 2013).

Figure 2 shows pH has a negligible effect on Se. The results of pH analysis are not in agreement with the study done by (Gedam et al. 2012). They have concluded pH has a large impact on Se, ignoring the fact that the other parameters (such as T or S0) need to be fixed during the pH analysis. As Fig. 2 shows when the other parameters are kept at a constant level, the impact of changing pH on Se is practically negligible. The pH performances of the other 6 membranes are exactly similar to Fig. 2. The main effective parameters that can change the efficiency (E) are: T, q, Re and the type of membrane used. Table 2 shows the variation of the parameters in this study.

Table 1 SWRO membranes used and their limitations

Used membranes	Max q_e (gpm)	Min q (gpm)	Max q (gpm)
SW30-2540	0.35	1	6
SW30HRLE-4040	1.06	3	16
SW30-4040	0.99	3	16
SW30-3031	0.53	3	9
SW30HR-380	4.75	15	64
SW30HRLE-440i	5.5	15	70.4
SW30 HRLE -400i	5	15	64
SW30 HRLE -1725	21.56	64.5	275.2

Data preparations

For each membrane type the first step is to adjust the feed water data, extracted from water library of ROSA under the name of "california.wat", which is shown in Table 3. Water temperature is 17 °C and SDI (silt density index), assumed to be under 5 (SDI <5) and (except for pH) the units of all parameters in Table 3 are in mgL^{-1}.

After processing feed water data in ROSA software, the other input parameters are: feed water flow (q), set at (approximately) half of maximum possible value of q (see Table 1) and Re as 15%. Then recovery percentage (Re) are changed by 1% at each time step from 1 to 15%

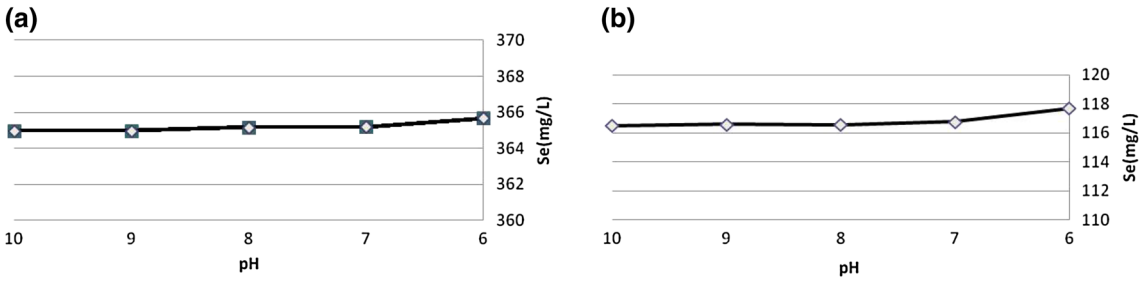

Fig. 2 Se variations caused by changes in pH. **a** Membrane type is SW30-2540, T = 20 °C, q = 1.3 gpm, Re = 15%, S0 = 32,000. **b** Membrane type is SW30hrle-1725, T = 25 °C, q = 120 gpm, Re = 10%, S0 = 32,000

Table 2 The range and amount of changes and parameter limits

Parameter	Range of parameter	Amount of change in each step
T°C	5–46	1@5–20, 2@20–46
TDS (S_0; mgL^{-1})	10,000–45,000	1000
Re (%)	1–15	1
q (gpm)	In possible range[a]	Depended on type

[a] See Table 1

Table 3 Default sea water properties (mg/l) that are used in this study

$NH_4 + + NH_3$	0.39	Ba	5	SO_4	1.5
K	262	CO_3	3.89	SiO_2	1
Na	6700	HCO_3	101	Boron	2.14
Mg	755	NO_3	0.5	CO_2	0.91
Ca	210	Cl	11,000	TDS	19,055.84
Sr	2.6	F	0.7	pH	7.9

(Fig. 3 zone A) for covering all possible ranges of q-Re combinations, or "q" and "Re" variations, and individually (Fig. 3 zone B), which should not reach more values than the ones shown in Table 1 such as q_e denoted as Eq. 2.

$$permeat.flow = effeluent.flow = q_e = \mathrm{Re} \times q \quad (2)$$

It is noticeable that the different shapes which are seen in zone(s) B of Fig. 3 are caused by different or irregular/random q-Re values assigned for each membrane. For covering the range of temperature, parameters reset on the default mode and only T can change in each time step from 5 to 46 °C (Fig. 3 zone C).Then the properties will return to default mode again. The variation of TDS is form 10,000 to 45,000 (mgL^{-1}). The concentrations of Na and Cl somehow are adjusted by relation between Na/Cl (in Table 3), so that the values are constant. To satisfy more practical conditions, temperature will change with TDS, while it can be calculated by Eq. 3. (Figure 3 zone D)

$$T = \begin{cases} 15\,^{\circ}\mathrm{C} \leftarrow TDS = 10000 + 3k \times 1000 \\ 20\,^{\circ}\mathrm{C} \leftarrow TDS = 10000 + (3k+1) \times 1000 \\ 25\,^{\circ}\mathrm{C} \leftarrow TDS = 10000 + (3k+2) \times 1000 \end{cases} \quad (3)$$

k is a natural number from 0 to 11. In each "step" input data such as S0, q, Re, T and Se are recorded in an EXCEL file. Figures 3, 4 show all the output data for 8 types of membranes. Table 4 shows the range of variation of the parameters that have been used for modeling and testing procedures.

Figures 3, 4 show all membranes have the same parametric variation or behavior corresponding to the variation of input parameters. Therefore, to show the relation between Se and other parameters we will focus on one of the membranes. And after developing the simulation equations, we can proceed with the calibration of other membranes.

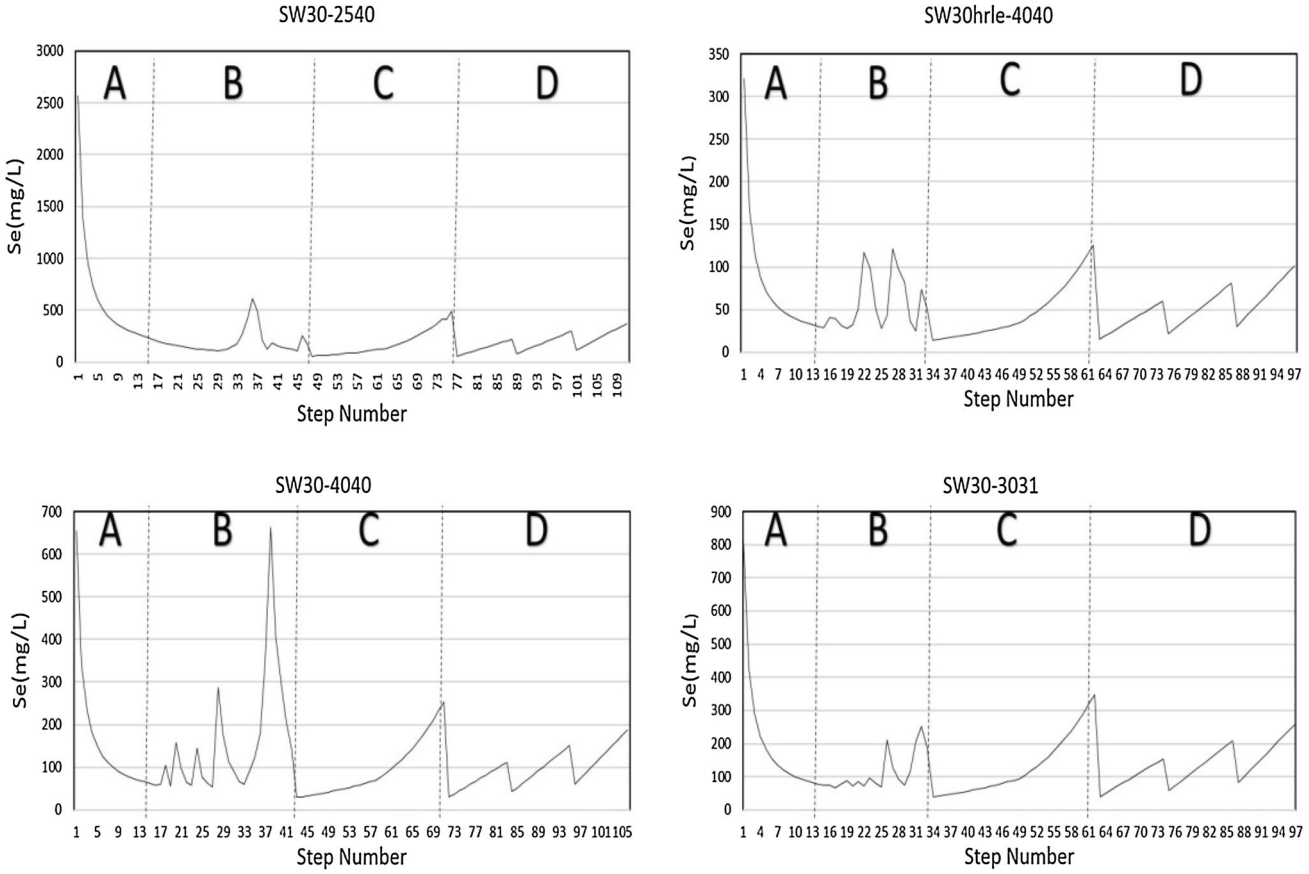

Fig. 3 The values of Se in different conditions for 4 SWRO membranes (2540, hrle4040, 4040, 3031 models)

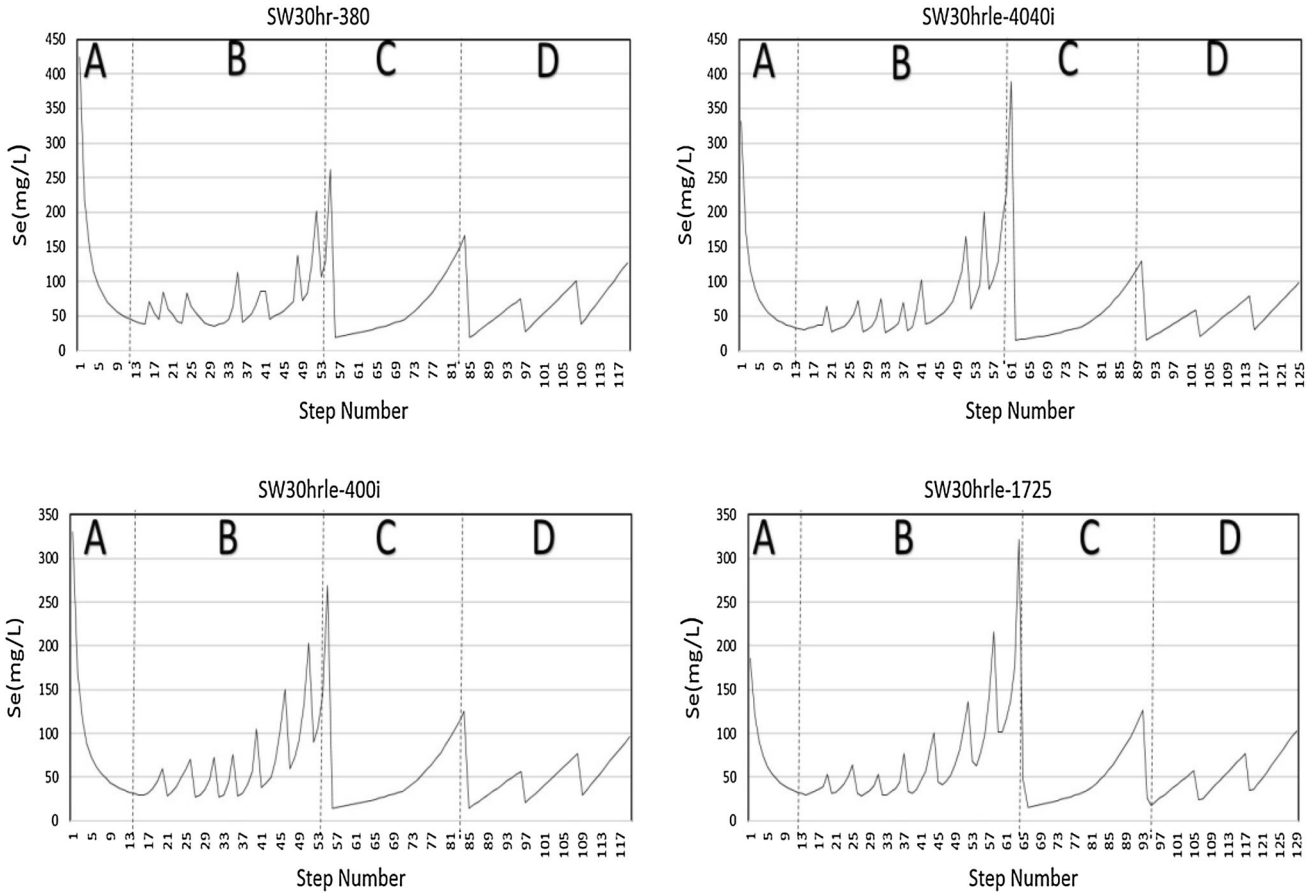

Fig. 4 The values of Se in different conditions for 4 SWRO membranes (hr380, hrle4040, hrle40i, hrle1725 models)

Table 4 The variation of parameters in each zone of Fig. 5

RO membrane	Parameter	A	B	C	D
SW30-2540	q (gal/m)	1	1–6	2.3	2.3
	Re %[a]	1–15	1–15	15	15
	Temp (°C)[a]	17	17	5–45	15–25
	S_0 (mg/L)[a]	19,057	19,057	19,057	10,000–42,000
	The zone data number	15	32	29	35
SW30hrle-4040	q (gal/m)	7	5–16	7	7
	The zone data number	15	18	29	35
SW30-4040	q (gal/m)	6	6–15	6.6	6.6
	The zone data number	15	27	29	35
SW30-3031	q (gal/m)	3.5	3–9	3.2	3.2
	The zone data number	15	19	27	35
SW30hr-380	q (gal/m)	30	15–64	30	30
	The zone data number	15	39	29	35
SW30hrle-440i	q (gal/m)	35	15–70	35	35
	The zone data number	15	46	29	35
SW30hrle-400i	q (gal/m)	32	15–64	33	33
	The zone data number	15	40	29	35
SW30hrle-1725	q (gal/m)	140	71.5–261.5	140	140
	The zone data number	15	51	29	35

[a] Variation of these parameters is similar for all 8 membranes

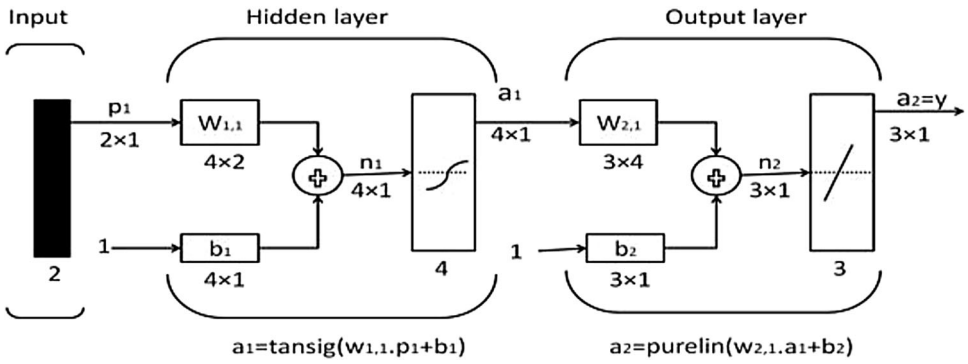

Fig. 5 A two layer feed-forward network

Mathematical modeling

In this study, the least squares method is used to solve the over constrained linear system to obtain the coefficients of the fitting polynomial (Venkatesan 2014). This method is based on linear algebra. Let y be the nth degree polynomial of x:

$$y_i = f(x_i, n) = \sum_{j=0}^{n} a_j \cdot x_i^n \tag{4}$$

where a_j(s) is coefficient of polynomial, Eq. 4 can be also expressed in form of a matrix:

$$\overbrace{\begin{bmatrix} a_0 & a_1 & \cdots & a_n \end{bmatrix}}^{A_{n+1}} \cdot \overbrace{\begin{bmatrix} x_1^0 = 1 & 1 & \cdots & 1 \\ x_1^1 & x_2^2 & \cdots & x_i^2 \\ \vdots & \vdots & \cdots & \vdots \\ x_1^n & x_2^n & \cdots & x_i^n \end{bmatrix}}^{X_{n+1,i}} = \overbrace{\begin{bmatrix} y_1 & y_2 & \cdots & y_i \end{bmatrix}}^{Y_i} \tag{5}$$

or

$$A_{n+1}.X_{n+1,i} = Y_i \quad or \; A.X = Y \tag{6}$$

For every matrix $X \in R^{n\times m}$, a unique matrix $X^+ \in R^{m\times n}$, which is called generalized (right) inverse exists satisfying (Karampetakis 1997):

$$X.X^+ = I_n \tag{7}$$

I_n: Identity matrix of size n. By multiplyingX^+ on (right hand of) both sides of Eq. 7 we have:

$$A.X.X^+ = A.I = A = Y.X^+ \tag{8}$$

And by this method 'A' which is a polynomial coefficients matrix, can be calculated. The analyses of the present study are performed using MATLAB software. The derived equation can be in the form of Eq. 4:

$$S_e = k.\frac{S_0.\alpha}{(q.\mathrm{Re})^{\theta}} \tag{9}$$

where k is a constant that depends on the type of the membrane; α, an "n" degree polynomial of T (Eq. 5); and θ, parameter that let us to calibrate the effect of (q.Re) for each membrane.

$$\alpha(T) = a_0 + a_1.T + a_2T^2 + \cdots + a_{n-1}.T^{n-1} + a_n.T \tag{10}$$

To evaluate k and θ for each membrane Eq. 6 is used, just when the temperature is equal to 17 °C (A, B zones in Fig. 3). In other words, we assume that α (17) = 1. In order to optimize the value ofθ, it can change from 0.50 to 2.00 by 0.01 steps to find out for what value of θ_i (s), k_i (s) has the relative minimum average absolute difference (RMAAD) with average k_i (Eq. 11–14).

$$k_i = \frac{(q.\mathrm{Re})^{\theta_i}}{S_0} \tag{11}$$

$$\theta_i = 0.50 + i \times 0.01 \tag{12}$$

$$average.k_i = \overline{k_i} = \frac{\sum_{j=1}^{t} k_{i,n}}{t} \tag{13}$$

$$RMADD_i = \frac{\sum_{j=1}^{t} \left|\overline{k_i} - k_{i,n}\right|}{t.\overline{k_i}} \tag{14}$$

where i: A natural number between 1 and 150; t: Number of existed steps in A and B zones in Figs. 3, 4; and $k_{i,n}$: k_i for step number "n", n varies between 1 and t. The best fit achieved and values of proper "i" and k for each membrane are shown in Table 4. Recognizing k and θ for each membrane and using data in zones C and D, the polynomial which best fits the T and α(T) is derived as Eq. 15, by MATLAB software. According to the calculations α will be in the form of Eq. 16:

$$\alpha(T) = \frac{S_{e,T}.(q.\mathrm{Re})^{\theta}}{k.S_0} \tag{15}$$

$S_{e,\,T}$ is the Se in temperature of T (°C); zones C and D of Figs. 3, 4.

$$\alpha = a_0 + a_1.T + a_2.T^2 \tag{16}$$

Table 5 Values of k, i, a0, a1, a2 for each membrane

	k	i	a_0	a_1	a_2
SW30-2540	0.002,218	39	0.527	−0.002	0.0018
SW30hrle-4040	0.001481	39	0.5957	−0.0096	0.0021
SW30-4040	0.002769	38	0.6077	−0.0086	0.0021
SW30-3031	0.002068	38	0.586	−0.0088	0.0021
SW30hr-380	0.007223	40	0.5971	−0.0095	0.0021
SW30hrle-440i	0.006498	40	0.5964	−0.0096	0.0021
SW30hrle-400i	0.005956	39	0.589	−0.0095	0.0021
SW30hrle-1725	0.022264	40	0.5955	−0.0096	0.0021

Values of a0, a1 and a2 for each membrane are shown in Table 5. The Se for each membrane is calculated by Eq. 16. Verification of Eq. 17 is shown in Table 8.

$$S_e = \frac{k.S_0}{(q.\mathrm{Re})^{0.5+i\times 0.01}}.(a_0 + a_1.T + a_2.T^2). \quad (17)$$

Neural network modeling

Artificial neural network (ANN) modeling is relatively a new method that is based on human's brain function of learning algorithms (Yi-Ming et al. 2004). Its priority is flexibility and capability of learning complex nonlinear/linear relations. MLF (multilayer feed-forward) networks trained with back-propagation algorithm are the most popular types of networks (Kabsch-korbutowicz and Kutylowska 2008; Salgado-Reyna et al. 2013; Svozil et al. 1997). We used MLF networks to make ANN models. The details of ANN structures and algorithms are briefly discussed by Ehteshami et al. (2016), Abraham (2005), Menhaj (2008), Salgado-Reyna et al. (2013). Basic architecture consists of three types of neuron layers such as input, hidden, and output layers. Figure 5 shows a two layer network. The signals flow from input to output units through feed-forward ANN networks, strictly in a form of feed-forward direction (Abraham 2005; Yang et al. 2009). The hidden layers consist of different number of neurons. In Fig. 5 parameters such as "a" is the output of neuron and "p" is the input. Parameters "w" and "p" are weight and bias, respectively, and all parameters denoted as matrices, and can be expressed as:

$$a = f(net) = f(n) = f(w^T.p + b) = f\left(\sum_{i=1}^{R} w_R^T.p_R + b\right) \quad (18)$$

$$p = [p_1, p_2, \ldots, p_R], w = [w_1, w_2, \ldots, w_R] \quad (19)$$

Figure 6 shows the most common "f" function. It transfers output of each layer to a simpler/more useful expression for calibrating the w_i and b_i (s) in next layer/step.

In order to train the function correctly, we must continue and repeat the process of calibrating and optimizing w_i, bi(s). The optimum of w_i, bi(s) will result in minimizing the mean square of error (MSE) value. This process will continue until we reach the required precision. In the following procedure, weights and biases will change every time that the process is repeated. The calibration process for w_i, b_i(s) is as (Alnaizy et al. 2013; Menhaj 2008; Salgado-Reyna et al. 2013):

$$w_{i,j}^{(l+1)} = w_{i,j}^{(l)} - \alpha \frac{\partial e(w,b)}{\partial w_{i,j}^{(l)}} \quad (20)$$

$$b_{i,j}^{(l+1)} = b_{i,j}^{(l)} - \alpha \frac{\partial e(w,b)}{\partial b_{i,j}^{(l)}} \quad (21)$$

$$\frac{\partial e(w,b)}{\partial w_{i,j}^{(l)}} = \left[\frac{1}{m}\sum_{i=1}^{m} \frac{\partial}{\partial w_{i,j}^{(l)}} e(w,b;x^{(i)},y^{(i)})\right] + \alpha w_{i,j}^{(l)} \quad (22)$$

$$\frac{\partial e(w,b)}{\partial b_{i,j}^{(l)}} = \left[\frac{1}{m}\sum_{i=1}^{m} \frac{\partial}{\partial b_{i,j}^{(l)}} e(w,b;x^{(i)},y^{(i)})\right] + \alpha b_{i,j}^{(l)} \quad (23)$$

where α is the learning rate. Figure 5 shows that outputs of previous layers will be the inputs of the neurons in the next layer and the result(s) of the output layer will be compared to the target values. In this study mean square of error (MSE) is the criterion for comparing the outputs.

$$mse = \frac{1}{m}\sum_{i=1}^{m} e^2 = \frac{1}{m}\sum_{i=1} (t - a_i)^2 \quad (24)$$

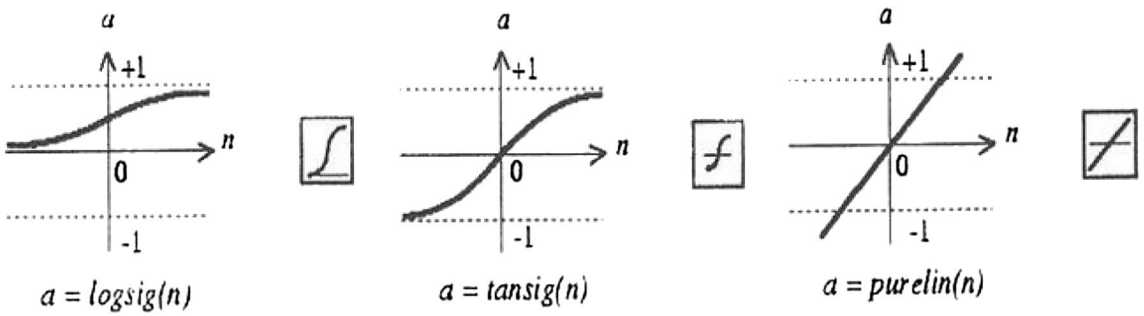

Fig. 6 Transfer functions

Table 6 Training parameters

α0	0.001	Network type	Feed-forward back-propagation
α decrees	0.1	Training function	Trainlm (Levenberg–Marquardt)
α increase	10	Adapting learning function	Train GDM
Maximum α	1E+10	Performance function	MSE
Min grad	1.00E–10	Transfer function	Tansign (x)

Table 7 Details of layers and neurons for each membrane

RO membrane	Number of hidden layers	Neurons in first layer	Neurons in second layer
SW30-2540	2	4	10
SW30hrle-4040	2	4	10
SW30-4040	2	5	8
SW30-3031	2	5	10
SW30hr-380	2	5	8
SW30hrle-440i	2	6	13
SW30hrle-400i	2	5	10
SW30hrle-1725	2	4	10

Table 8 Comparing models and Eq. 17 results to (existed) real data (Figs. 3, 4)

RO	Average (real) Se (mgL^{-1})	MAE for models (mgL^{-1})	R for models (%)	MAE for Eq. 17 (mgL^{-1})	R for Eq. 17 (%)
SW30-2540	249.6	5.95	97.03	9.46	96.52
SW30hrle-4040	54.97	1.46	96.92	1.67	96.71
SW30-4040	120.34	3.39	96.73	5.54	95.38
SW30-3031	138.01	3.04	97.43	4.91	96.33
SW30hr-380	71.41	2.01	97.33	2.5	96.27
SW30hrle-440i	62.05	2.15	96.33	2	96.38
SW30hrle-400i	58.68	1.99	96.88	1.84	96.64
SW30hrle-1725	58.78	1.83	96.73	2.1	96.21

where t_i is target (real) value data and a_i is the network output.

Two feed-forward with back propagation learning rule (Eqs. 20–23) are used to develop the models in MATLAB environment. Design parameters of the networks have been represented in Tables 6, 7.

Data and models

Input data are parameters such as T, Re, q and target(output) data will be Se/S0. Table 7 shows the model properties for each membrane. To obtain a better precision, values shown in Figs. 3, 4 were multiplied by 10, with simple interpolation of existing data (Figs. 3, 4). Table 7 shows number of hidden layers and number of neurons in each layer.

Results and discussion

Table 8 shows the precision of equation (Eq. 17) for each membrane. Both (NN models) and Eq. 17 are verified by the initial input data (Fig. 3). The resulted or simulated $\overline{S_e}$, are compared to Se values of (Figs. 3, 4). For a better understanding of both MAE and R, values are shown in Table 8.

$$MAE = \frac{\sum_{i=1}^{t} \left| S_e - \overline{S_e} \right|}{t} \tag{25}$$

$$R = 100 \times \frac{\sum_{i=1}^{t} \left[1 - \frac{\left| S_e - \overline{S_e} \right|}{S_e} \right]}{t} \tag{26}$$

$$Error = \left(1 - \frac{\text{Model result}}{\text{Real data}} \right) \times 100 \tag{27}$$

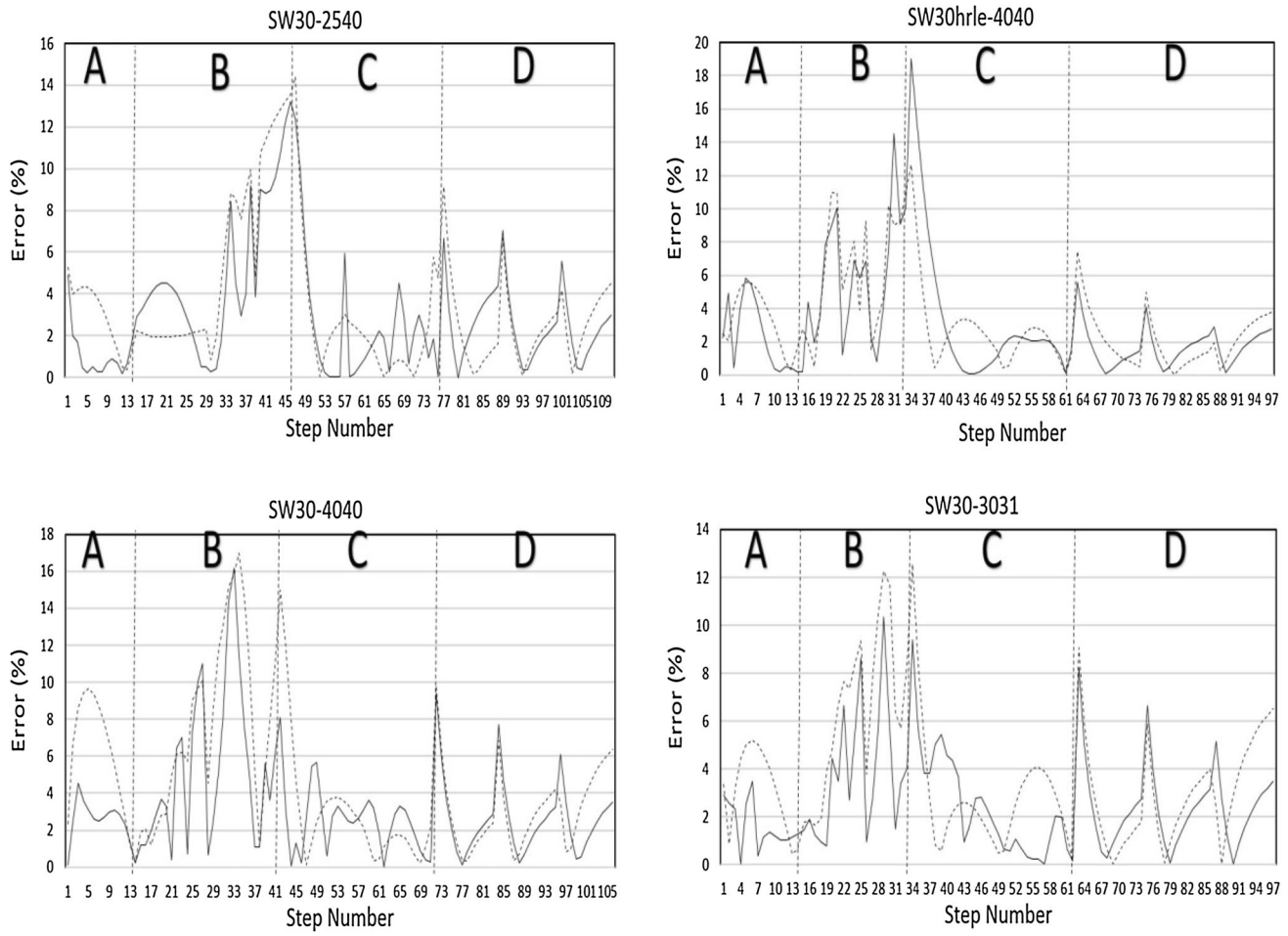

Fig. 7 The errors of mathematical equations and models procedure for selected 4 SWRO membranes, (2540, hrle4040, 4040, 3031 models)

where t is the number of existing data for each membrane (Figs. 3, 4) and $\overline{S_e}$ is the simulated Se with models and/or Eq. 17. The error values as calculated by Eq. 27 are shown in Fig. 6.

Table 8 shows that both models and Eq. 17 are reliably accurate and the ANN models even have a slightly higher precision comparing to Eq. 17. Figures 7, 8 illustrate the model verification results based on the simulated data. The dashed lines show mathematical models errors and simple lines show ANN models errors.

Conclusions

In this study an effective mathematical equation was developed as a simple expression, such as Eq. 17. Presented formula can be used/calibrated for other types of membranes. Both Eq. 17 and models are reliable to predict RO system performance, and design parameters such as S_0, T, Re and p. Furthermore, it can be used to optimize the process of desalination systems. The effects of pressure and/or the other design and operating parameter(s) of membranes structure can be added by other researchers to the Eq. 17 and models. Therefore, the main highlight of this study was to develop a model to simulate 8 types of RO membranes that are able to cover a wide range of feed water and operational conditions. Main advantages of the mathematical modeling are: (1) simplicity of expression/proving and using them and (2) the form of solutions and its sensitivity toward two/multi parameter that can be observed and analyzed. The advantages of ANN modeling are: (1) ability of modeling of complex relationships which is not possible for model with ordinary mathematical methods; (2) in most cases ANN models have higher precision compared with mathematical methods; (3) ANN models can be adapted with new data and upgraded with them; (4) best combination of design parameters in ANN models can be achieved by try and error method. This process also revealed that the number of (hidden layers) and their neurons should be chosen wisely, both lack and excess of it, may decrease the model precision. One of the most important finding in this study is when the number of data is sufficient for modeling the precision of

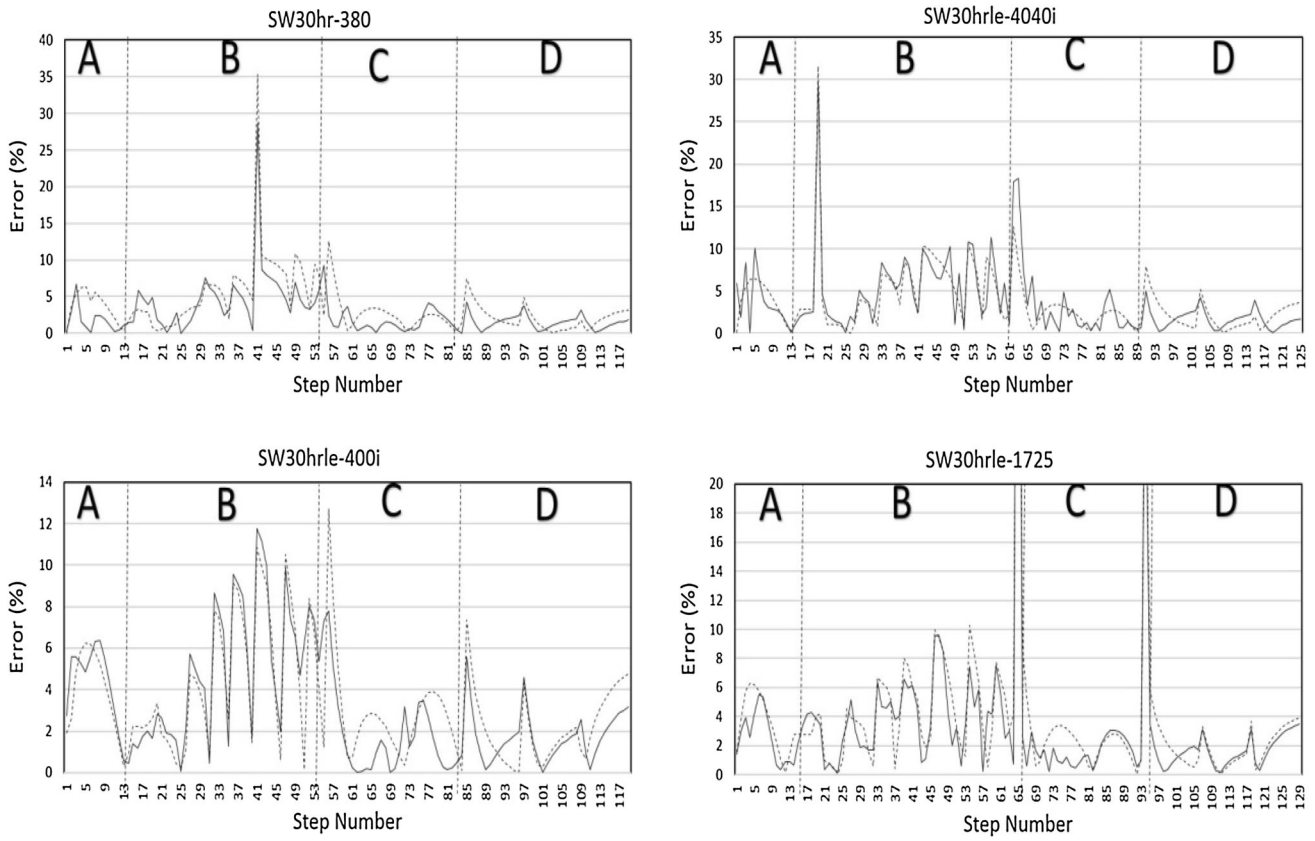

Fig. 8 The errors of mathematical equations and models procedure for selected another 4 SWRO membranes (hr380, hrle4040i, hrle400i, hrle1725 models)

model is directly depended on (and limited by) data that are being used. In other word the most important uncertainty would be caused by uncertainty of input data. This means that even if we use the other methods of modeling (such as genetic algorithm, dynamic NN, etc.), better result will not be achieved because, errors depend on error of data that are used for making the models.

Acknowledgements The authors are grateful to the Dow Chemical Company; for providing required data, documents and Model; "Reverse Osmosis System Analysis" ROSA. We also wish to thank Dr. Rabbani for his technical and logistical assistance in modeling and analysis works.

References

Abbasi Maedeh P, Mehrdadi N, Nabi Bidhendi GR, Zare Abyaneh H (2013) Application of artificial neural network to predict total dissolved solids variations in groundwater of Tehran Plain, Iran. Int J Environ Sustain 2(1):10–20

Abraham A (2005) Artificial neural networks. Handbook of measuring system. Oklahoma State University, Stillwater, pp 901–908 **(elements: B—signal conditioning)**

Afrasiabi N, Ehteshami M, Ardakanian R (2009) Optimum design of RO membrane by using simulation techniques. J Desalination Water Treat 9(1–3):189–194

Al-Mutaz IS (2003) Hybrid RO MSF: a practical option for nuclear desalination. Int J Nucl Desalination 1:1–10

Alnaizy R, Aidan A, Abachi N, Jabbar NA (2013) Neural network model identification and advanced control of a membrane biological reactor. J Membr Sep Technol 2(4):231–244

Altaee A (2012) A computational model to estimate the performance of 8 inches RO membranes in pressure vessel. J Membr Sep Technol 1(1):60–71

Arulchinnappan S, Rajendran G (2011) A study on reverse osmosis permeating treatment for yarn dyeing effluent using fuzzy linear regression model. Afr J Biotechnol 10(78):17969–17972

Carter NT (2015) Desalination and membrane technologies: federal research and adoption issues. Congressional Research Service 7-5700, 1–18. http://www.crs.gov

Chen J, Li G (2005) Marine reverse osmosis desalination plant a case study. J Desalination 174(3):299–303

Clayton R (2011) A review of current knowledge. Desalination for water supply. Foundation of water research, Bucks

Crittenden J, Trussell RD, Hand K, Tchobanoglous G (2005) Water treatment principles and design, 2nd edn. Wiley, Jersey City, pp 3–18

Ebrahimi A, Ehteshami M, Dahrazma B (2015) Isotherm and kinetic studies for the biosorption of cadmium from aqueous solution by Alhaji maurorum seed. Process Saf Environ Prot 98:374–382

Ehteshami M, Biglarijoo N (2014) Determination of nitrate concentration in groundwater in agricultural area in Babol County, Iran. Iran J Health Sci 2(4):1–9

Ehteshami M, Peralta RC, Eisele H, Deer H, Tindall T (1991) Assessing pesticide contamination to ground water: a rapid approach. J Ground Water 29(6):862–886

Ehteshami M, Farahani ND, Tavassoli S (2016) Simulation of nitrate contamination in groundwater using artificial neural networks. J Model Earth Syst Environ 2(1):1–10

Garud RM, Kore SV, Kulkarni GS (2011) A short review on process and applications of reverse osmosis. Univ J Environ Res Technol 1(3):233–238

Gedam VV, Patil JL, Kagney S, Sirsam RS, Labhasetwar P (2012) Performance evaluation of polyamide reverse osmosis membrane for removal of contaminants in ground water collected from Chandrapur district. J Membr Sci Technol 2(3):1–5

Greenlee LF, Lawler DF, Freeman BD, Marrot B, Moulin P (2009) Reverse osmosis desalination: water sources, technology, and today's challenges. Water Res 43:2317–2348

Harrak El, Elazhar N, Zdeg F, Zouhri AA, Elazhar N, Elmidaoui MA (2013) Performances analysis of the reverse osmosis desalination plant of brackish water used for irrigation: case study. Am J Appl Chem 1(3):43–48

Hiroki M (2010) Design of a desalination plant, Department of technology and built environment, University of Gavle. Bachelor's Thesis in Industrial Engineering, pp 1–35

Jafar MM, Zilouchian A (2002) Prediction of critical desalination parameters using radial basis functions networks. J Intel Rob Syst 34(2):219–230

Jiang A, Ding Q, Wang J, Jiangzhou S, Cheng W, Xing C (2014) Mathematical modeling and simulation of SWRO process based on simultaneous method. J Appl Math 11, Art ID 908569. doi:10.1155/2014/908569

Kabsch-korbutowicz M, Kutyłowska M (2008) The possibilities of modelling the membrane separation processes using artificial neural networks. Environ Prot Eng 34(1):15–36

Karampetakis NP (1997) Computation of the generalized inverse of a polynomial matrix and applications, vol 252(1–3). Elsevier Science Inc, Amsterdam, pp 35–61

Kumar RM, Saravanan K (2011) Application of reverse osmosis membrane system for treatment of effluent in textile knitted fabric dyeing. Afr J Biotechnol 10(70):15756–15762

Libotean D, Giralt J, Giralt F, Rallo R, Wolfe T, Cohen Y (2009) Neural network approach for modeling the performance of reverse osmosis membrane desalting. J Membr Sci 326(2):408–419

Menhaj MB (2008) Fundamental of neural network, vol 1. Industrial Amir Kabir University, Tehran

Nakayama A, Sano Y (2013) An application of the Sano-Nakayama membrane transport model in hollow fiber reverse osmosis desalination systems. Desalination 311:95–102

Pangarkar BL, Sane MG, Guddad M (2011) Reverse osmosis and membrane distillation for desalination of groundwater: a review. Int Sch Res Netw Mater Sci 9, Art ID 523124. doi:10.5402/2011/523124

Patroklou G, Sassi KM, Mujtaba IM (2013). Simulation of boron rejection by seawater reverse osmosis desalination, Aidic conference series, pp 1–10

Radu AI, van Vrouwenvelder JSM, Loosdrecht MC, Picioreanu C (2010) Modeling the effect of biofilm formation on reverse osmosis performance: flux, feed channel pressure drop and solute passage. J Membr Sci 365:1–15

Reverse Osmosis System Analysis, ROSA, The Dow Chemical Company (2015). http://www.dow.com/en-us/water-and-process-solutions/resources/design-software/rosa-software

Salami Shahid E, Ehteshami M (2015) Simulation, evaluation and prediction modeling of river waterquality properties (case study: Ireland Rivers). Int J Environ Sci Technol 12(10):3235–3242

Salami Shahid E, Ehteshami M (2016) Application of artificial neural networks to estimating DO and salinity in San Joaquin River basin. Desalination Water Treat 57(11):4888–4897

Salgado-Reyna A, Soto-Regalado E, Gómez-González R, Cerino-Córdova FJ, Garza-González MT, García-Reyes, Alcalá-Rodríguez MM (2013) Artificial neural networks for modeling the reverse osmosis unit in a wastewater pilot treatment plant. J Desalination and Water Treatment. 53:1177–1187

Svozil D, Kvasnieka V, Pospichal J (1997) Introduction to multi-layer feed-forward neural networks. Chemo metr Intel Lab Syst 39:43–62

Venkatesan R (2014) Comparison between LTTD and RO process of sea-water desalination: an integrated economic. Environ Ecol Framew Curr Sci 106(378):3

Williams ME (2003) A brief review of reverse osmosis membrane technology. EET Corporation and Williams Engineering Services Company, Inc, Harriman, pp 1–29

Stover R (2013) New high recovery reverse osmosis water treatment for industrial, agricultural and municipal applications. The International Desalination Association World Congress on Desalination and Water Reuse, Tianjin, pp 1–10

Yang ZP, Lu WX, Long YQ, Li P (2009) Application and comparison of two prediction models for groundwater levels: a case study in Western Jilin Province, China. J Arid Environ 73:487–492

Yi-Ming K, Chen-Wuing L, Kao-Hung L (2004) Evaluation of the ability of an artificial neural network model to assess the variation of groundwater quality in an area of black foot disease in Taiwan. Water Res 38:148–158

Zirakrad A, Hashemian SJ, Ghaneian MT (2013) Performance study of reverse osmosis plants for water desalinationin Bandar-Lengeh, Iran. J Commun Health Res 2(1):8–14